Received: 17 February 2020 | Accepted: 4 August 2020

DOI: 10.1002/pros.24064

ORIGINAL ARTICLE

The Prostate WILEY

Inflammatory infiltration is associated with AR expression and poor prognosis in hormone naïve prostate cancer

Milly McAllister PhD[1] | Vera Constâncio MSc[1] | Samantha Patek PhD, MBChB[1] | Hao W. G. Gan MBChB[1] | Peter Bailey PhD[2] | Helen Wheadon PhD[3] | Mark Underwood PhD, MBChB[4] | Hing Leung PhD, MBChB[2,4] | Joanne Edwards PhD[1]

[1]Unit of Gastrointestinal Cancer and Molecular Pathology, Institute of Cancer Sciences, College of Medical, Veterinary, and Life Sciences, University of Glasgow, Glasgow, UK

[2]Cancer Research UK Beatson Institute, Glasgow, UK

[3]Paul O'Gorman Leukaemia Research Centre, University of Glasgow, Glasgow, UK

[4]Department of Urology, Queen Elizabeth University Hospital, Glasgow, UK

Correspondence
Milly McAllister, PhD, Unit of Gastrointestinal Cancer and Molecular Pathology, Institute of Cancer Sciences, College of Medical, Veterinary, and Life Sciences, University of Glasgow, Glasgow G61 1QH, UK.
Email: m.mcallister.1@research.gla.ac.uk

Funding information
Prostate Cancer UK, Grant/Award Number: S14-003

Abstract

Background: Tumor microenvironment inflammatory infiltration is proposed as a pro-tumorigenic mechanism for prostate cancer with proinflammatory cytokines stimulating androgen receptor (AR) activity. However, association with patient prognosis remains unclear. This study derives an inflammatory gene signature associated with AR expression and investigates CD3+ and CD8+ T-lymphocyte infiltration association with AR and prognosis.

Methods: Gene profiling of inflammatory related genes was performed on 71 prostate biopsies. Immunohistochemistry on 243 hormone-naïve prostate cancers was performed for CD3, CD8, AR, and phosphorylated AR tumor expression.

Results: Multiple proinflammatory genes were differentially expressed in association with high *AR* expression compared with low *AR* expression including *PI3KCA* and *MAKP8* (adjusted $P < .05$). High CD3+ and high CD8+ infiltration associated with reduced cancer-specific survival ($P = .018$ and $P = .020$, respectively). High CD3+ infiltration correlated with high tumor cytoplasmic AR expression and if assessed together, they associated with reduced cancer-specific and 5-year survival from 90% to 56% ($P = .000179$). High CD8+ cytotoxic infiltration associated with high androgen-independent tumor nuclear AR serine 213 phosphorylation (correlation coefficient = 0.227; $P = .003$) and when assessed together associated with poor clinico-pathological features including perineural invasion ($P = .001$). Multiple genes involved in proinflammatory signaling pathways are upregulated in high *AR* expressing prostate samples.

Conclusion: T-lymphocyte infiltration in hormone-naïve disease associates with androgen-independent driven disease and provides possible therapeutic targets to reduce transformation from hormone-naïve to castrate-resistant disease.

KEYWORDS

androgen receptor, inflammation, phosphorylation, prostate cancer, T-lymphocytes

1 | INTRODUCTION

Androgens activating the androgen receptor (AR) play a crucial role in the development of 80% to 90% of prostate cancers (CaP). AR activation via induction of AR phosphorylation at serine 81 (pAR^{ser81})[1-4] promotes cell proliferation and reduces cell death, therefore current therapies aim to inhibit AR activation directly or via depletion of androgens by androgen deprivation therapy (ADT). However, despite 10-year survival rates tripling over the past 40 years in the UK, over 300,000 men worldwide still die each year from CaP due to late stage diagnosis and development of castrate-resistant disease. This highlights the need to understand the pathogenesis and progression of CaP further.[5] In addition to classical AR activation, the AR can be activated independent of androgens through numerous pathways including phosphatidylinositol-3-kinase (PI3K)/AKT, onterleukin-6 (IL-6)/Janus kinase (JAK)/signal transducer and activator of transcription (STAT), and Ras/Raf/mitogen-activated protein kinase (MAPK) which result in AR phosphorylation to promote transcriptional activity, protein stability and the development of castrate-resistant disease.[4] For example, phosphorylation of the AR at Serine 213 via PI3K/AKT signaling results in activation of the AR via an androgen independent mechanism, the PI3K/AKT pathway through loss of phosphatase and tensin homolog (PTEN) is upregulated in 40% to 70% of CaPs.[6,7]

The prostate is an immune-competent organ composed of infiltrating immune cells including macrophages, dendritic cells, B-lymphocytes, and T-lymphocytes. Inflammatory changes observed in CaP include increased inflammatory cell infiltration and proinflammatory cytokine expression, which promote multiple signaling pathways linked with CaP development, such as PI3K/AKT and IL-6/JAK/STAT.[8] It is hypothesized that these proliferative conditions promote the dedifferentiation of prostate epithelial cells, activation of AR signaling, and ultimately CaP development.

In CaP, the adaptive immune response is highly active and prominent including cytotoxic T-lymphocytes, helper T-lymphocytes, and regulatory T-lymphocytes. CD4+ helper T-lymphocytes induce (TNF)-related apoptosis, with a reduction in CD4+ infiltration in CaP, when compared with benign prostatic hyperplasia and prostatic intraepithelial neoplasia, associating with poor clinico-pathological features including high Gleason sum and elevated prostate specific antigen (PSA) concentration.[9] Additionally, regulatory T-cells (Tregs) suppress and regulate T-lymphocytes, with elevated Tregs within the tumor microenvironment reducing the antitumor effects of T-lymphocytes. However, in CaP elevated Treg infiltration associates with reduced cancer specific survival (CSS) in CaP.[10,11] One cell type regulated by Tregs are CD8+ cytotoxic cells which destroy microbes and cancer cells via cytokine release, Fas signaling, or the perforin pathway. In colorectal cancer, high CD8+ infiltration is associated with favorable clinical outcomes and can be modulated to increase its cytotoxic functions via immune checkpoint inhibitors which target programmed cell death protein 1 or anti-cytotoxic-T-lymphocyte-associated protein 4 (CTLA4). However, in CaP these immune checkpoint inhibitors have shown little effect with high immune checkpoint blockage resistance, with over expression of AR significantly reducing CD8+ infiltration, PC-1 and CTLA-4 expression, an correlating with tumor progression, increased serum PSA concentration, and the presence of metastases.[12] Interestingly, loss of PTEN, a common feature in CaP, is associated with increased CD8+ infiltration and reduced time to biochemical relapse, highlighting interesting links between inflammation and AR. However, contradictory reports have been published for each inflammatory cell type depending on disease stage, tissue location, AR expression and cytokine expression. Ultimately, further research is required to identify important players of inflammatory driven CaP and potential therapeutic targets or synergistic drug combinations. Therefore, we aimed to derive an inflammatory gene expression signature associated with high AR expression within a prostate biopsy and establish if this signature is associated with more aggressive disease. Furthermore, we aimed to determine the relationship between local adaptive immune cell infiltration in hormone naive CaP and AR/phosphorylated AR expression.

2 | METHODS

2.1 | Patient biopsy cohort

Prostate biopsies from 71 patients were collected between 2007 and 2012 via trans-rectal ultrasound (TRUS) guided biopsies and snap frozen upon extraction. Ethical approval was gained from the Multicentre Research Ethics Committee for Scotland (MREC/01/0/36) and Local Research and Ethics Committees. An anonymized database was available containing clinical information with all patient identifiers removed and included age at biopsy, diagnosis, Gleason sum, serum PSA concentration, and presence of metastases.

2.2 | Gene expression analysis

RNA was extracted from frozen TRUS biopsies using the RNease Mini kit (Qiagen, UK). Biopsies were minced in RNA lysis buffer lysis buffer and centrifuged in QiaShredder columns (Qiagen, UK) for 2 minutes. Samples were transferred to a RNeasy mini column with 70% ethanol and centrifuged for 30 seconds. Samples were washed in RW1 buffer followed by RNA wash buffer with ethanol buffer via centrifugation for 30 seconds and eluted in RNase free water. Each sample RNA was reverse-transcribed by adding 1 μL oligo (dT) and 1 μL dNTPmix for 5 minutes at 65°C. Each sample was then added to 4 μL 5X first strand buffer, 0.5 μL water, 0.5 μL SuperScript III reverse transcriptase, 1 μL 0.1 M DTT, and 1 μL RNaseOUT and incubated for 30 minutes at 50°C followed by 15 minutes at 70°C (Invitrogen, UK). Ninety-six primer pairs (Table S1) were pooled together and 0.5 μL primer mix was added to each sample along with 2.5 μL TaqMan PreAmp Master Mix (Thermo Fisher Scientific, UK), and 0.75 μL water. These primers were pre-selected based on their applicability across a range of cancers, prostatic diseases, and inflammatory processes. Samples were vortexed, centrifuged, and placed in a

thermocycler for 10 minutes at 95°C, 10 to 14 cycles for 15 seconds at 95°C, and 4 minutes at 60°C. Samples underwent exonuclease treatment by adding 0.2 μL exonuclease I reaction buffer, 0.4 μL exonuclease I, and 1.4 μL water and incubating for 30 minutes at 37°C and 15 minutes at 80°C (New England Biolabs, UK). Each sample was diluted in five-fold in TE buffer, added to 3 μL 2X SsoFast EvaGreen Supermix (Bio-Rad, UK) and 0.3 μL 20X DNA Binding Dye sample loading reagent (Fluidigm, UK), and vortexed and centrifuged. Individual primer pairs were added to 2.5 μL 2X assay loading reagent and 2.25 μL 1X DNA suspension buffer. Each individual primer pair and sample was loaded into a 96.96 Dynamic Array IFC (Fluidigm) and run on the Fluidigm Biomark HD system (Table S2).

2.3 | Immunohistochemistry

In total, 243 patients diagnosed with CaP were recruited from the Greater Glasgow and Clyde Health Board between 2008 and 2009 (Biobank ethical approval for use of tissue, GG&C health board ethics number 10/50704/60, Safe Haven ethical approval for use of clinical information, GG&C health board ethics number 12/WS/0142). An anonymized database was available containing clinical information with all patient identifiers removed and included Gleason sum, serum PSA concentration, presence of metastases, perineural invasion, serum albumin concentration, C-reactive protein concentration, hormonal therapy, time to biochemical relapse, and time to cancer specific death. All samples were gathered via trans-ultrasound guided biopsies.

Immunohistochemistry was performed for AR, pAR^{ser81}, AR 213 phosphorylation (pAR^{ser213}), Ki67 proliferation index, CD3, and CD8. Sections were dewaxed in histoclear, rehydrated through graded alcohol, and heated under pressure for 5 minutes in Tris-ethylenediaminetetraacetic acid (Tris-EDTA) (5 nM Trizma Base, 1 mM EDTA, pH8 or 9) for antigen retrieval. Sections were placed in 3% H_2O_2 for 30 minutes and blocked for 30 minutes in 1.5% or 5% horse serum in Tris-buffered saline. Antibodies for AR (M3562; Dako, UK), pAR^{ser81} (07-1375; Millipore, UK), Ki67 (Clone MIB-1; Dako), CD3 (RM-9107-S; Thermo Fisher Scientific, UK), and CD8 (Clone C8/114b; Dako) were incubated overnight at 4°C diluted at 1:100, 1:1000, 1:1000, 1:1000, and 1:200 respectively. Antibody for pAR^{ser213} (IMG-561; Imgenex, UK) was incubated for 1 hour at room temperature diluted at 1:100. EnVision (Dako) or ImmPRESS detection kit (Vector Laboratories, UK) was used to detect bound antibodies followed by 3,3-diaminobenzidine tetrahydrochloride (DAB, Dako). Samples were counterstained and dehydrated before being mounted with Di-*N*-butylephthalate in xylene (DPX). Slides were scanned and visualized using Hamamatsu NanoZoomer (Welwyn Garden City, UK) and Slidepath Digital Image Hub, version 4.0.1 (Leica Biosystems, UK). Staining intensity for AR, pAR^{ser81}, and pAR^{ser213} was performed using a weighted histo-score method for both nuclear and cytoplasmic expression. In brief, the score was calculated by sum of (1X % cells staining weakly positive) + (2X % cells staining moderately positive) + (3X % cells staining strongly positive) with a maximum of 300 (100% strongly stained) and a minimum of 0 (100% with no staining). Ki67, CD3, and CD8 expression was performed by counting positive cells within three representative 0.6 × 0.6 mm intratumoural areas. Tissue staining intensity and positive cell counts were scored by two independent observers.

2.4 | Statistical analysis

Statistical analysis was performed using SPSS version 22 for Windows. Interclass correlation coefficients confirmed the weighted histoscores and positive cell counts were consistent between two independent observers. Receiver operator characteristic (ROC) curve analysis was employed to determine high and low thresholds. CSS from diagnosis was analyzed using Kaplan Meier log-rank analysis from date of diagnosis to date of death from CaP. Cox-regression, χ^2 analysis, Pearson's rank correlation, and Mann-Whitney *U* tests were performed. Gene expression analysis performed using R. Delta cycle thresholds values for each biopsied sample were quantile normalized using the R package limma.[13] Hierarchical clustering (Ward.D2) of the normalized expression data was then performed identifying two broad clusters. Genes differentially expressed (DE) between clusters were then identified using the R package limma.[13] Heatmaps visualizing DE genes were generated using the R/Bioconductor package ComplexHeatmap.[14] Gene set enrichment analysis was performed using the R/Bioconductor packages clusterProfiler[15] and ReactomePA.[16] Regression analysis was performed using the lm function form R package stats and the results plotted using R package ggplot2. Boxplots were generated using the R package ggpubr with significant difference between distributions calculated using the Kruskal-Wallis test.

3 | RESULTS

3.1 | Inflammatory gene expression in prostate cancer

Inflammatory gene expression profiling was performed on 71 frozen TRUS prostate biopsies taken to diagnose a patient's prostatic disease to determine an inflammatory gene signature and whether this associates with high AR expression (Table S3). Unsupervised hierarchal clustering separated the 71 prostate biopsies into two distinct classes (Figure 1A). Class 1 contained 11 patients of which 45.5% were CaP, 45.5% were benign, and 9% were prostate intraepithelial neoplasia (PIN). Patients in class 1 were diagnosed with CaP at a median age of 69 years (interquartile range [IQR]: 67-71 years) with a median Gleason sum of 7 (IQR: 6-7) and a median PSA concentration of 8.9 ng/mL (IQR: 5.8-17.1 ng/mL) at time of biopsy. Class 2 contained 60 patients of which 23.3% were CaP, 31.7% were benign, and 5% were PIN. Patients in class 2 were diagnosed with CaP at a median age of 69.5 years (IQR: 62.3-74 years) with a median Gleason sum of 7 (IQR: 7-7) and a median PSA concentration of 12.7 ng/mL (IQR: 9.1-27.8 ng/mL) at time of biopsy.

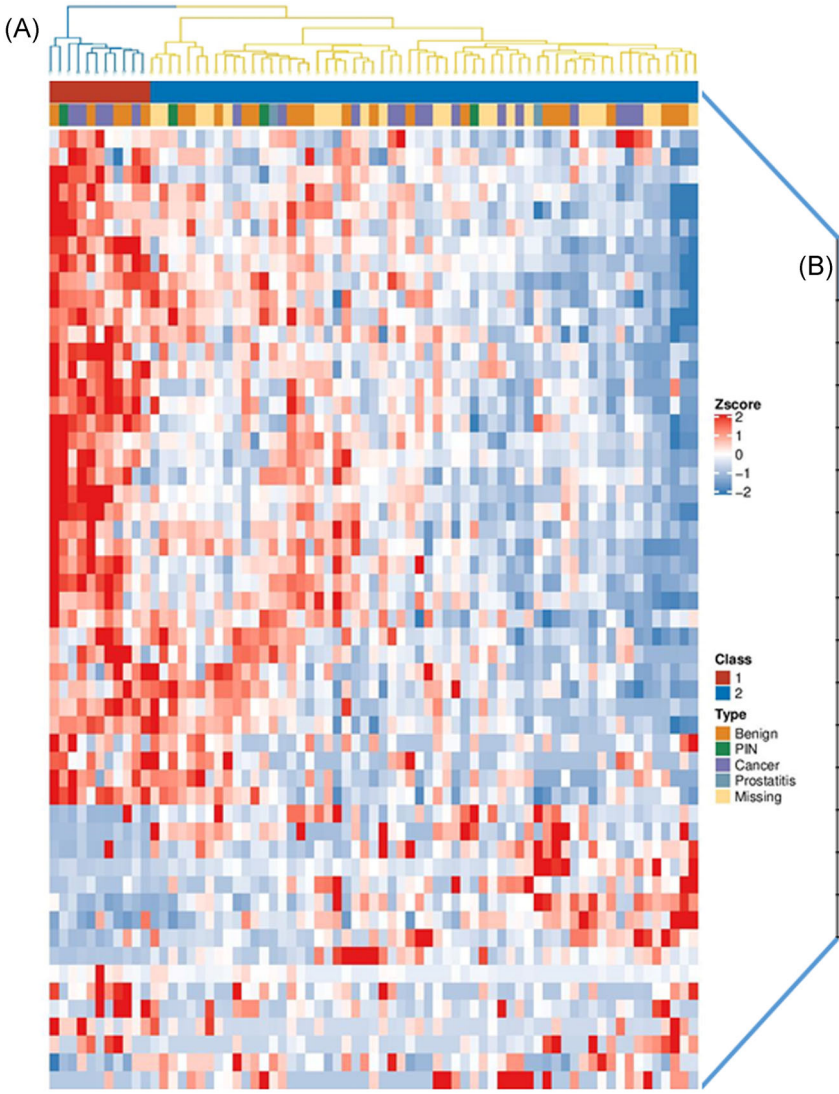

(B) DE genes in cancer only samples

Gene Name	Log 2 Fold Change in Expression	Adjusted P Value
NFKB1	1.9	0.0018
ERB2	1.9	0.0018
EGFR	1.9	0.0018
PLCB3	1.8	0.0018
ITGB1	1.8	0.0018
KLK3	1.8	0.0018
AKT1	1.8	0.0023
PI3CA	1.7	0.0023
LTA4H	1.7	0.0023
CASP1	1.7	0.0037
IKBKB	1.7	0.0038
CACNA1C	1.6	0.0038
BCL2L1	1.6	0.0038
IL1R	1.6	0.0038
STAT3	1.6	0.0039

FIGURE 1 Differential gene expression analysis between patients from the frozen trans-rectal ultrasound (TRUS) biopsy cohort by Fluidigm array analysis. A, Heatmap demonstrating differentially expressed (DE) genes between all class 1 and all class 2 patients ($P < .05$). B, Table of top 15 DE expressed genes between cancer class 1 and cancer class 2 patients ordered by adjusted *P* value. Adjusted *P* value (*P*adj) < .05 used for significant DE genes

AR gene expression was trending towards being expressed higher in class 1 biopsies compared with class 2 biopsies, however this was not significant (Kruskal-Wallis $P = .051$). Interestingly, the gene for AR regulated PSA, *KLK3*, was significantly highly expressed in class 1 samples versus class 2 (Kruskal-Wallis $P = 2.2 \times 10^{-5}$). In total, 54 out of 96 genes were computed as DE in class 1 versus class 2 biopsies, with the majority of upregulated genes being proinflammatory and protumorigenic including *KLK3*, *EGFR*, *CASP1*, *TGFB1*, *PI3CA*, *MAPK14*, and *NF-ℓB* (adjusted *P* value [padj] < .05) (Figure 1). Furthermore, gene set enrichment analysis highlighted multiple pathways significantly enriched in class 1 versus class 2 samples. Among the enriched pathways, those relating to signaling by IL (20 genes) and IL-4 and IL-13 signaling (11 genes) were the most significant (padj < 1×10^{-12}) (Figure 2).

Subsequently, when the 19 CaP samples were selected for, these samples fell into the same two classes as identified following gene clustering analysis (Table S4). 26 out of the 96 genes were significantly DE in cancer class 1 versus cancer class 2 of which 25 were upregulated (Figure 1B). All genes DE in the cancer class 1 overlap with the genes identified in all class 1 samples (Table S5). Despite *AR* gene expression not being statistically different between cancer class 1 compared with cancer class 2 (Kruskal-Wallis $P = .15$) (Figure S1A), *KLK3* was significantly higher in cancer class 1 versus cancer class 2 (Kruskal-Wallis $P = .0016$) (Figure S1B). Interestingly, 6 out of the 26 gene expression profiles identified in both all class 1 samples and cancer class 1 samples significantly correlated with higher AR expression including *PI3CA*, *ERB3*, *IL1R*, *MAPK1*, *MAPK8*, and *PSMA* ($P < .05$) (Figure S1C-H).

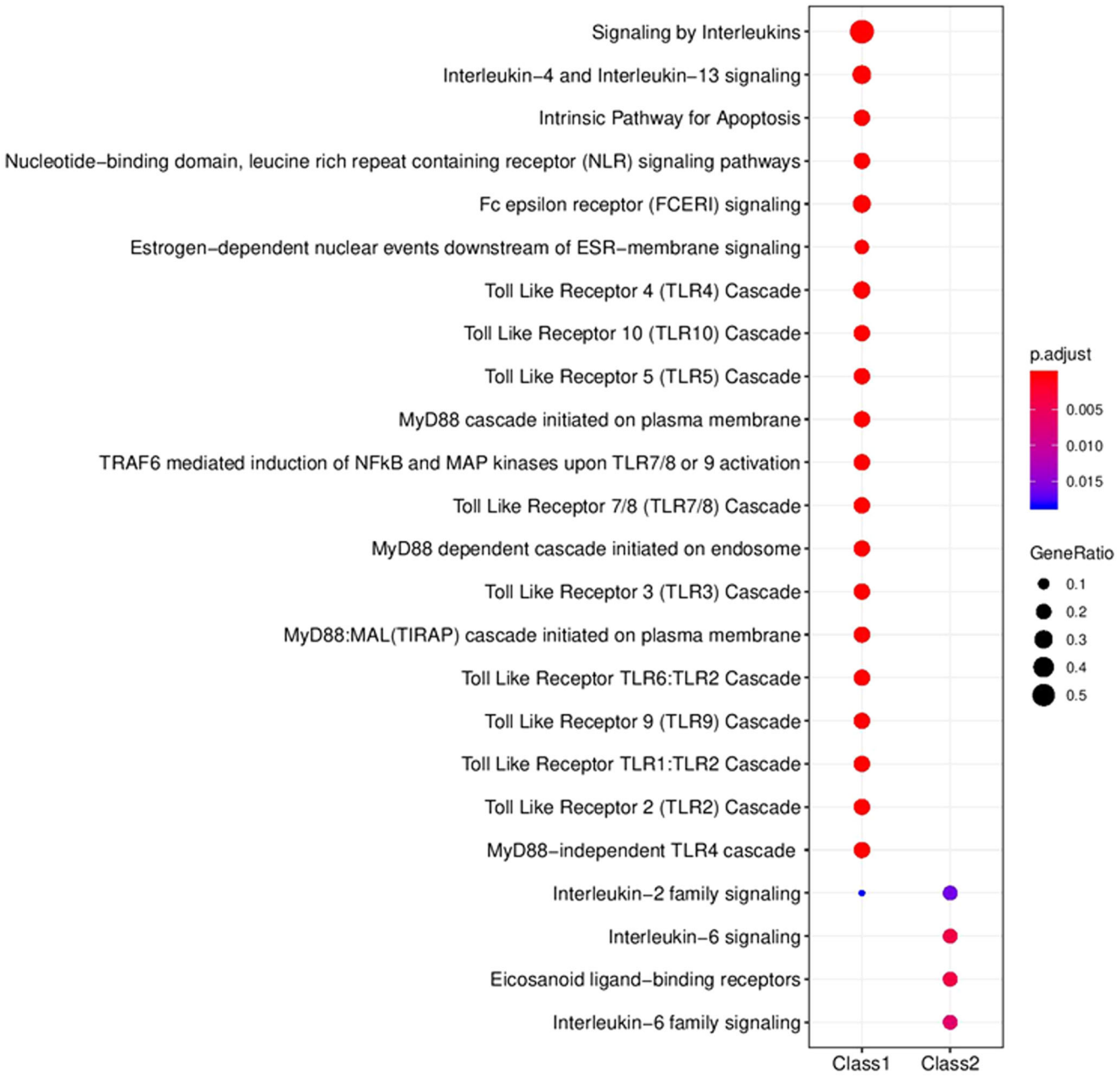

FIGURE 2 Gene set enrichment analysis between class 1 and class 2 samples from the frozen TRUS biopsy cohort by Fluidigm array analysis. Dot plot demonstrates the enriched pathways in class 1 samples compared with class 2 samples with color chart representing significance of enriched pathways and circumference of dot representing the gene ratio. MAP, mitogen-activated protein; NF-κB, nuclear factor κB; TRUS, trans-rectal ultrasound

3.2 | Clinico-pathological characteristics

Analysis was performed on 243 hormone-naïve CaP patients, with clinico-pathological features and associations with CSS and the development of biochemical relapse seen in Table 1. Patient characteristics included age, Gleason sum, serum PSA concentration, presence of metastases, perineural invasion, serum albumin concentration, C-reactive protein concentration, time to biochemical relapse, hormonal therapy receive, and time to cancer specific death. At diagnosis, high Gleason sum (>7) ($P < .0001$), high serum PSA concentration (>20 ng/mL) ($P = .000419$), presence of metastasis ($P < .0001$), perineural invasion ($P = .006$), and high albumin concentration ($P = .001$) was associated with decreased CSS. Thirty-eight patients developed biochemical relapse with a mean time to biochemical relapse of 2.20 years (IQR: 1.08-2.90 years). The development of biochemical relapse significantly associated with reduced CSS ($P = .000067$). Eighty-one patients died from CaP with a mean time to death of 4.90 years (IQR: 4.50-5.73 years).

TABLE 1 Clinico-pathological cohort characteristics and relationship with clinical outcome measures in 243 patients diagnosed with prostate cancer and recruited from the Greater Glasgow and Clyde Health Board between 2008 and 2009; the number of patients in each group are described along with the significance to cancer specific survival (CSS) and time to biochemical relapse (R); Kaplan Meier survival curves with log-rank tests were considered significant if $P < .05$

Clinico-pathological characteristics	Patient numbers n (%), total n = 243	Clinical outcome significance
Gleason sum (<7/7/>7/missing)	76 (31.3%), 85 (35.0%), 60 (24.7%), 22 (9.1%)	CSS: $P < .00001$ R: $P = .871$
Serum PSA concentration (ng/mL) (<10/10-20/>20/missing)	76 (31.3%), 53 (21.8%), 101 (41.6%), 13 (5.3%)	CSS: $P = .000419$ R: $P = .649$
Metastases (No/yes/missing)	132 (54.3%), 62 (25.5%), 49 (20.2%)	CSS: $P < .00001$ R: $P = .209$
Biochemical relapse (No/yes/missing)	135 (55.6%), 38 (15.6%), 70 (28.8%)	CSS: $P = .000067$
Hormonal therapy (No/yes/missing)	67 (27.6%), 134 (55.1%), 42 (17.3%)	CSS: $P = .047$
Perineural invasion (No/yes/missing)	115 (47.3%), 99 (40.7%), 29 (11.9%)	CSS: $P = .006$ R: $P = .094$
Albumin, g/L (<35, >35, missing)	19 (7.8%), 170 (70%), 54 (22.2%)	CSS: $P = .001$ R: $P = .720$
C-reactive protein, mg/L (<10, >10, missing)	61 (25.1%), 41 (16.9%), 141 (58.0%)	CSS: $P = .113$ R: $P = .461$

Abbreviation: PSA, prostate specific antigen.

3.3 | Androgen receptor and AR phosphorylation expression analysis

As AR expression at the messenger RNA level associated with expressions of inflammatory genes, we investigated if AR expression and phosphorylation status associated with inflammatory cell infiltrate in the tumor and microenvironment. Tumor cytoplasmic (TC) AR expression ranged from 0 to 233 weighted histoscore units (WHU) with a median of 76 WHU (IQR: 40-100). ROC curve analysis determined a threshold of 83 WHU that separated TC AR expression into high and low. TC AR expression significantly associated with reduced CSS ($P = .001$; hazard ratio [HR] = 7.135 [95% confidence interval {CI}: 2.304-22.091]) and stratified 5-year survival from 68% (low expression) to 50% (high expression) but was not associated with time to biochemical relapse ($P = .758$; HR = 0.941 [95% CI, 0.419-2.110]). TC AR expression associated with Gleason sum, serum PSA concentrations, metastases, and perineural invasion at diagnosis following χ^2 analysis (Figure 3A,B).

TC pAR^{ser81} expression ranged from 0 to 197 WHU with a median of 100 WHU (IQR: 100-120). ROC curve analysis determined a threshold of 110 WHU that separated TC pAR^{ser81} expression into high and low. pAR^{ser81} expression significantly associated with reduced CSS ($P = .046$; HR = 1.950 (95% CI, 1.066-3.567)) and stratified 5-year survival from 65% (low expression) to 46% (high expression) but was not associated with time to biochemical relapse ($P = .911$; HR = 1.439 [95% CI, 0.492-4.206]). Expression of TC pAR^{ser81} expression did not associate with any clinico-pathological features following chi-squared analysis (Figure 3C,D).

TC pAR^{ser213} expression ranged from 0 to 203 WHU with a median of 100 WHU (IQR: 93-122). ROC curve analysis determined a threshold of 99 WHU that separated TC pAR^{ser213} expression into high and low. TC pAR^{ser213} expression was not associated with reduced CSS ($P = .093$; HR = 2.100 [95% CI, 0.441-1.921]) or time to biochemical relapse ($P = .513$; HR = 0.472 [95% CI, 0.153-1.456]). Expression of TC pAR^{ser213} expression did not associate with any clinico-pathological features following χ^2 analysis (Figure 3E,F).

3.4 | Inflammatory cell infiltration expression

CD3+ T-lymphocyte infiltration count ranged from 0 to 274 positive cells with a median of 68 (IQR: 44-105). ROC curve analysis determined a threshold of 60 positive cells that separate CD3+ infiltration into high and low (Figure 4A). CD3+ infiltration was associated with reduced CSS ($P = .018$; HR = 1.383 [95% CI, 0.591-3.236]) and stratified 5-year survival from 69% (low infiltration) to 54% (high infiltration) (Figure 5A). CD3+ T-lymphocyte infiltration was associated with Gleason sum and perineural invasion at diagnosis following χ^2 analysis and positively correlated with elevated TC AR expression (Pearson's correlation coefficient (c.c) = 0.278, $P = .000232$) (Table 2 and Figure S2D). High CD3+ infiltration, when combined with high TC AR expression associated with reduced CSS when compared with low expression

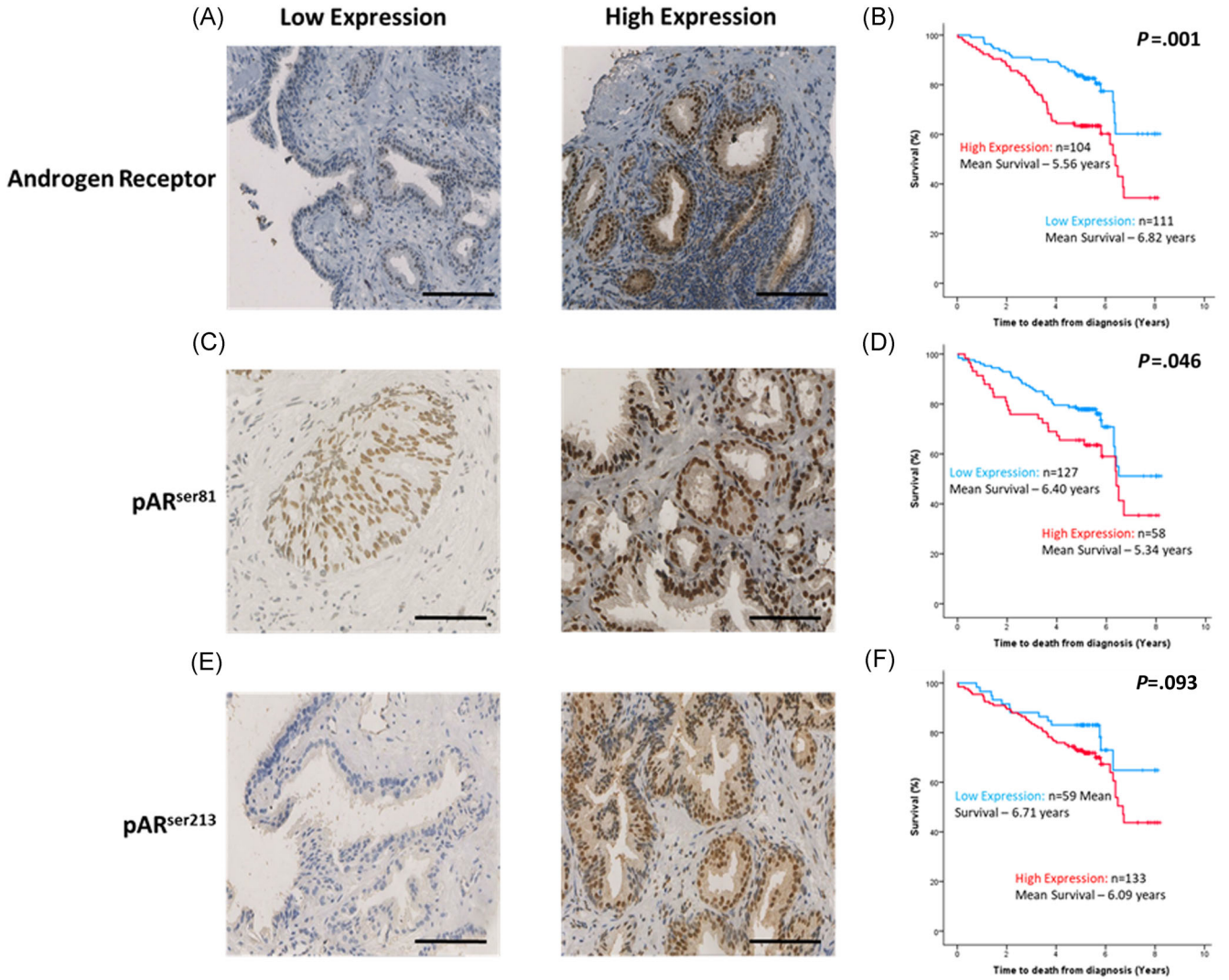

FIGURE 3 Androgen receptor (AR) and AR phosphorylation in 243 hormone-naïve prostate cancer patients diagnosed with prostate cancer and recruited from the Greater Glasgow and Clyde Health Board between 2008 and 2009. A, Low and high tumor cytoplasmic AR expression. B, High tumor cytoplasmic AR expression associated with reduced cancer specific survival. C, Low and high tumor cytoplasmic pAR^{ser81} expression. D, High tumor cytoplasmic pAR^{ser81} expression associated with reduced cancer specific survival. E, Low and high tumor cytoplasmic pAR^{ser213} expression. F, pAR^{ser213} expression was not associated with cancer specific survival within this cohort. Scale bars represent 100 μm and censor lines indicate loss of patient follow-up. pAR^{ser81}, androgen receptor serine 81 phosphorylation; pAR^{ser213}, androgen receptor serine 213 phosphorylatio

(*P* = .000179; HR = 2.118 [95% CI, 1.427-3.144]) and reduced 5-year survival from 90% (low expression) to 56% (high expression), and associated with poor clinic-pathological features including Gleason sum, PSA concentration, metastases, perineural invasion, development of biochemical relapse, and highly proliferative Ki67+ tumors (*P* = .000026, *P* = .025, *P* = .001, *P* = .000043, *P* = .022, and *P* = .000349, respectively) (Figure 5B).

Furthermore, cytotoxic CD8+ T-lymphocyte infiltration count ranged from 3 to 36 positive cells with a median of 15 (IQR :11-19). ROC curve analysis determined a threshold of 13 positive-cells that separated CD8+ infiltration into high and low (Figure 4B). CD8+ infiltration was associated with reduced CSS (*P* = .020; HR = 2.121 [95% CI, 0.773-5.817]) and stratified 5-year survival from 66% (low infiltration) to 53% (high infiltration) (Figure 5C). CD8+ T-lymphocyte infiltration was associated with Gleason sum, serum PSA concentration, and perineural invasion at diagnosis and positively correlated with TC AR expression (c.c = 0.247, *P* = .001) (Table 2 and Figure S2A). High CD8+ infiltration, when combined with high TC AR expression associated with reduced CSS when compared with low expression (*P* = .000257; HR = 1.945 [95% CI, 1.356-2.790]) and 5-year survival was reduced from 81% (low expression) to 57% (high expression). Additionally, high CD8+ infiltration combined with high TC AR expression was associated with Gleason sum, PSA concentration, metastases, perineural invasion, development of biochemical relapse, and highly proliferative Ki67+ tumors (*P* = .000208, *P* = .000226, *P* = .016, *P* = .000017, *P* = .002, and *P* = .000263, respectively) (Figure 5D). Interestingly, cytotoxic CD8+ T-lymphocyte infiltration did not

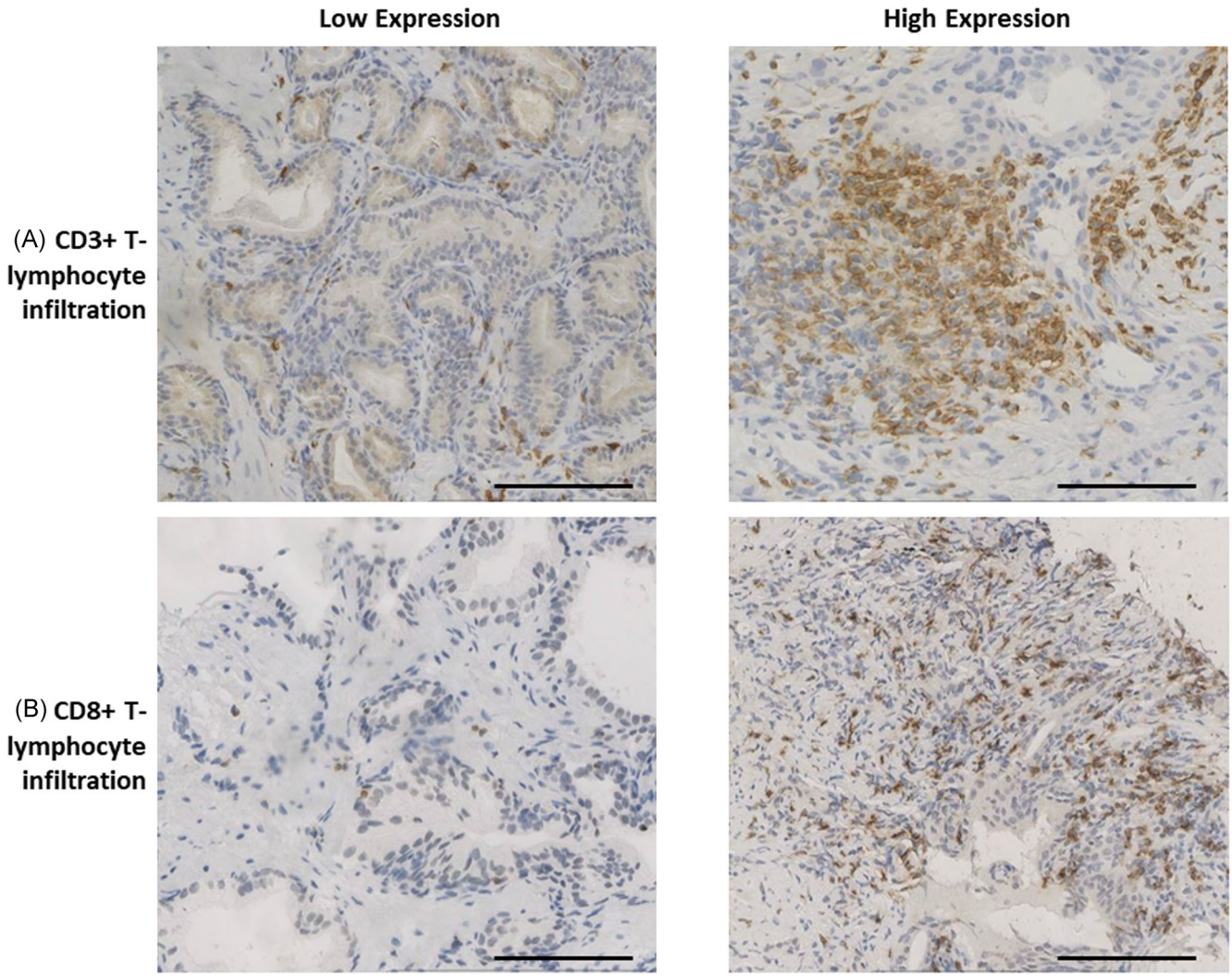

FIGURE 4 Low and high T-lymphocyte infiltration into the tumor microenvironment of 243 hormone naïve prostate cancer specimens diagnosed with prostate cancer and recruited from the Greater Glasgow and Clyde Health Board between 2008 and 2009. A, Low and high CD3+ T-lymphocyte infiltration. B, Low and high CD8+ T-lymphocyte infiltration. Scale bars represent 100 μm

correlate with androgen driven pAR^{ser81} within the cytoplasm or nucleus of tumor cells (c.c = 0.152, $P = .054$ and c.c = 0.024, $P = .762$, respectively) (Table 2). However, CD8+ T-lymphocyte infiltration significantly correlated with androgen-independent AKT driven pAR^{ser213} within the cytoplasm and nucleus (c.c = 0.185, $P = .015$ and c.c = 0.227, $P = .003$, respectively) (Table 2 and Figure S2B,C). High CD8+ T-lymphocyte infiltration combined with high tumor nuclear pAR^{ser213} expression is significantly associated with poor clinico-pathological features including perineural invasion following chi-squared analysis ($P = .001$).

4 | DISCUSSION

Elevated inflammatory cells within the peripheral zone of the prostate are linked with the development of CaP (relative risk = 1.3, 95% confidence interval = 1.10-1.54).[8,17] With this in mind, we investigated how T-lymphocyte infiltration associated with cancer specific survival and the AR and the prognostic use of this for patients with Ca. Additionally, we aimed to investigate if a single TRUS biopsy could be used to identify aggressive characteristics in CaP. We found multiple proinflammatory genes DE in prostate biopsies including *NFκB* which has previously been reported to be upregulated in CaP and seen to promote increased cellular proliferation, ADT resistance, and induce antiapoptotic signals.[18-21] Furthermore, we observed significant T-lymphocyte infiltration in hormone-naïve CaP and a reduction in cancer specific survival which associated with high AR expression and androgen-independent AR serine 213 phosphorylation.

In contrast to our findings, many claim that inflammatory cell infiltration delivers a protective environment and reduces the risk of CaP.[22,23] This is further reflected in various other cancers including colorectal cancer and renal cell carcinoma whereby studies into modulating the immune response to provoke an antitumour effects

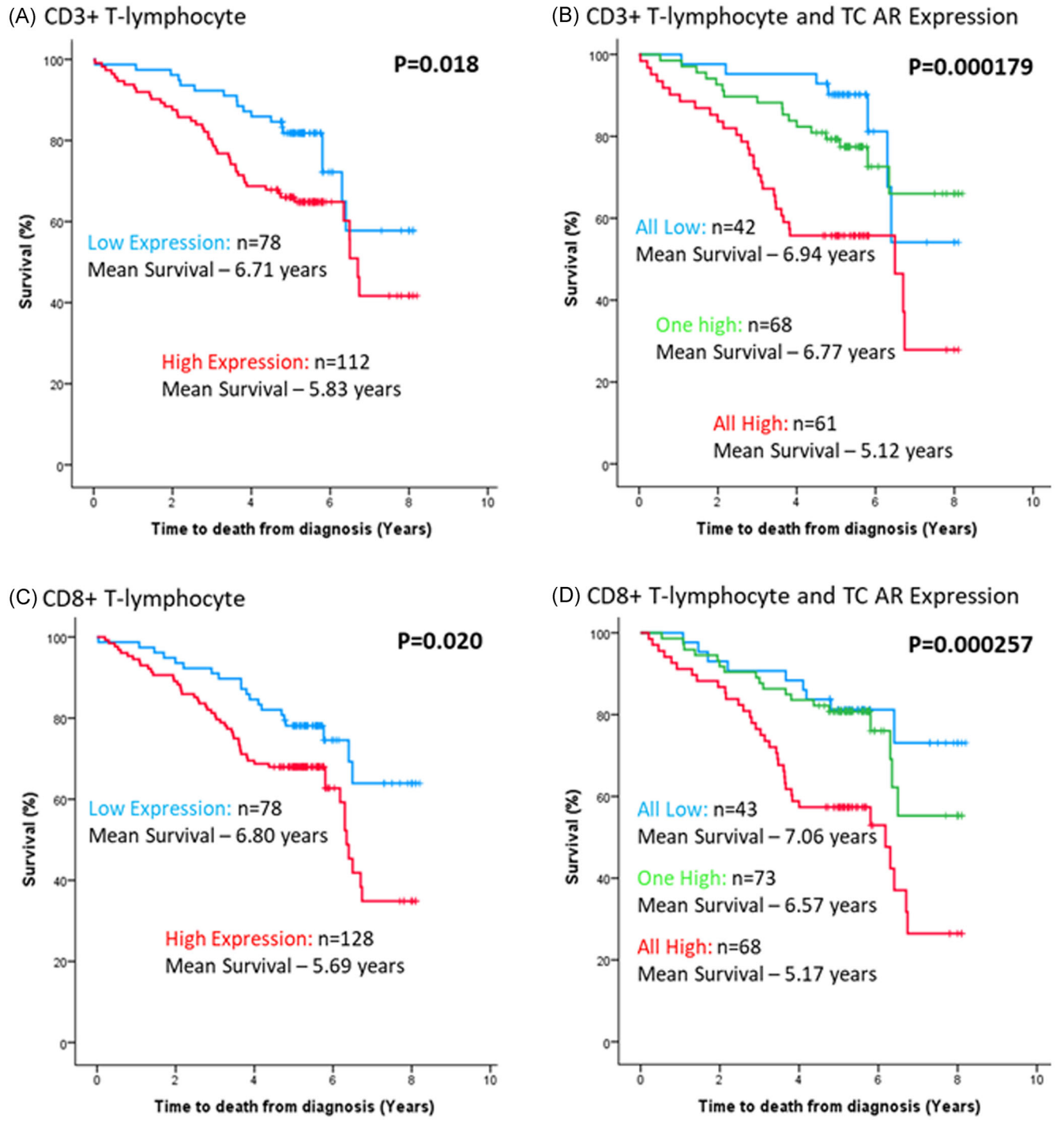

FIGURE 5 T-lymphocyte infiltration in prostate cancer and association with androgen receptor expression in 243 patients diagnosed with prostate cancer and recruited from the Greater Glasgow and Clyde Health Board between 2008 and 2009. A, CD3+ T-lymphocyte infiltration reduced survival from 6.71 to 5.83 years. B, High CD3+ infiltration and high tumor cytoplasmic androgen receptor expression reduced survival from 6.94 to 5.12 years. C, CD8+ T-lymphocyte infiltration reduced survival from 6.80 to 5.69 years. D, High CD8+ infiltration and high tumor cytoplasmic androgen receptor expression reduced survival from 7.06 to 5.17 years. Censor lines indicate loss of patient follow-up

have proved successful.[24,25] However, contradictory studies, in conjunction with our own, have identified a protumorigenic response associated with local inflammatory infiltration within the tumor microenvironment. Chronic inflammation within the prostate is linked with the dedifferentiation of the prostatic epithelium and protumourigenesis with multiple pathways dysregulated that alter the tumor microenvironment and provide a highly proliferative environment for CaP.[26,27] Interestingly, in CaP it is hypothesized that it

TABLE 2 Correlation between CD8+ T-lymphocyte and CD3+ T-lymphocyte infiltration and AR phosphorylation status in 243 patients diagnosed with prostate cancer and recruited from the Greater Glasgow and Clyde Health Board between 2008 and 2009

AR status	Correlation with CD8+ T-lymphocyte infiltration (C.c [*P* value])	Correlation with CD3+ T-lymphocyte infiltration (C.c [*P* value])
AR tumor nuclear	0.088 (.237)	−0.002 (.984)
AR tumor cytoplasmic	**0.247** (**.001**)	**0.278** (**.000232**)
pAR^{ser81} tumor nuclear	0.024 (.762)	−0.013 (.875)
pAR^{ser81} tumor cytoplasmic	0.152 (.054)	0.116 (.168)
pAR^{ser213} tumor nuclear	**0.227** (**.003**)	0.107 (.188)
pAR^{ser213} tumor cytoplasmic	**0.185** (**.015**)	0.101 (.214)

Note: C.c, Pearson's correlation coefficient. Bold values represents significant *p*-values.
Abbreviation: AR, androgen receptor.

is the pro-inflammatory cytokines secreted by local inflammatory infiltrate, such as IL-6, IL-8, and TNF-α that stimulates AR signaling independent of androgens for example via JAK-STAT, RAS-RAF-MAPK, PI3K-AKT, and nuclear factor B (NF-κB) pathways.[28]

Following unsupervised hierarchal clustering of the frozen TRUS prostate biopsies, two classes separated the cohort into patients expressing significantly higher *KLK3* expression in class 1 and lower *KLK3* expression in class 2 ($P = .016$). We discovered 54 genes were DE in class 1 samples versus class 2 samples including the overexpression of *MAPK14*, a key mediator of MAPK signaling implicated in controlling cell death and survival.[29,30] Upregulation of MAPK signaling as a result of IL-6 is involved in the development of castrate resistant CaP.[31] Furthermore, Wegiel et al also identified IL-6 activated PI3K signaling in CaP, in which we interestingly found a key member of this signaling pathway, *PI3KCA*, differentially and over expressed in class 1 high *KLK3* expressing biopsies. Additionally, overexpression of *NFκB* was observed in high *KLK3* expressing biopsies, a gene involved in regulating IL-8 expression and promoting chemotaxis. Upregulation of this gene and NF-κB/RELA signaling is observed following androgen stimulation of androgen-dependent LNCaP cells.[18] However, contradictory to our findings of *CASP-1* overexpression, downregulation of caspase-1 is observed in breast cancer, and when knocked out provided a highly proliferative environment for colon epithelial cells and the development of colon tumors.[32-34] Interestingly, when we analyzed only those patients who were diagnosed with CaP, all DE genes in cancer class 1 were also DE in all samples in class 1 including *EGRF*, *AKT1*, *CASP-1*, and *NFκB*. Furthermore, we found multiple genes including *PI3CA*, *PSMA*, *ERB3*, and *IL1R* all to significantly correlate with increased *AR* expression, a poor prognostic marker of CaP. Therefore, we decided to explore how T-Lymphocyte infiltration within the tumor microenvironment was associated with CaP specific survival and if it associated with AR expression.

Steiner et al reported a significant increase in infiltrating CD3+ cells in benign prostatic hyperplasia when compared with normal to the normal prostate.[35] However, contradictory to this, high CD3+ infiltrating T-cells have a positive prognostic effect in many cancers.[36] We observed high CD3+ T-lymphocyte infiltration significantly reduced cancer specific survival in hormone-naïve CaP ($P = .018$). Furthermore, this correlated with high TC AR expression (c.c = 0.278 and $P = .000232$) and when patients expressed high CD3+ infiltration and high AR expression, cancer specific survival reduced significantly. However, Patnaik et al identified that following blocking AR with a DNA vaccine in androgen sensitive mice, CD3+ T-cell infiltration increased and prolonged CaP recurrence.[37] Additionally, we explored how CD8+ cytotoxic T-cells effects survival and discovered high CD8+ infiltration reduced cancer specific survival and associated with high TC AR expression. High CD8+ and high AR expression significantly reduced survival from 7.06 to 5.17 years. However, conflicting results have been observed in triple negative breast cancer, with high CD8+ T-cell infiltration reducing breast cancer mortality.[38] In many cancers, high CD8+ infiltration is a favorable prognostic marker, with many immunotherapies aiming at stimulating CD8+ anti-tumoural behavior via anti-CTLA4 or anti-PDL1 immunotherapies. As such, in some cancers the lack of an intratumoural immune niches of stem-like CD8 T-cells is associated with more progressive disease.[39] Interestingly, high CD8+ infiltration also associated with high pAR^{ser213} expression in hormone-naïve tumors. Serine 213 is a known site for AKT binding and becomes activated via the PI3K/AKT cascade which is regulated by PTEN, a tumor suppressor commonly deleted or mutated in 30% of primary and 100% of metastatic CaP.[40,41] When patients express a loss of PTEN this associates with elevated CD8+ infiltration in the prostate tumor microenvironment and significantly reduces time to recurrence from diagnosis.[12] However, the mechanism though which loss of PTEN stimulates CD8+ infiltration remains unclear.

Together, our results have provided evidence that levels of T-cells in CaP microenvironment are associated with poor prognosis. Controversial results have been demonstrated here suggesting a poor prognostic effect of T-lymphocyte infiltration in hormone-naïve disease and a strong association between AR expression as well as androgen-independent AR activation. However, how this is reflected in castrate resistant disease is critical to provide prevention and further therapeutic options for this lethal form of CaP.

ACKNOWLEDGMENT

This work was funded by Prostate Cancer UK.

CONFLICT OF INTERESTS

The authors declare that there are no conflict of interests.

AUTHOR CONTRIBUTIONS

MM performed experiments, analyzed data and wrote manuscript. VC performed immunohistochemistry for CD3. SP collected all patient information and developed the cohort of samples used for immunohistochemistry analysis within this study. HG assisted with immunohistochemistry. PB assisted with bioinformatic analysis. HW helped design Fluidigm experiment. MU aided in project design and the gathering of prostate biopsy material. HL aided in project design. JE helped with all aspects of the manuscript including project design and execution.

ETHICS STATEMENT

Multicentre Research Ethics Committee for Scotland (MREC/01/0/36) and Local Research and Ethics Committees.

ORCID

Milly McAllister http://orcid.org/0000-0003-4952-8255

REFERENCES

1. Attar RM, Takimoto CH, Gottardis MM. Castration-resistant prostate cancer: locking up the molecular escape routes. *Clin Cancer Res*. 2009;15(10):3251-3255.
2. Brennen WN, Isaacs JT. Cellular origin of androgen receptor pathway-independent prostate cancer and implications for therapy. *Cancer Cell*. 2017;32(4):399-401.
3. Edwards J, Krishna NS, Mukherjee R, Watters AD, Underwood MA, Bartlett JM. Amplification of the androgen receptor may not explain the development of androgen-independent prostate cancer. *BJU Int*. 2001;88(6):633-637.
4. Chen S, Xu Y, Yuan X, Bubley GJ, Balk SP. Androgen receptor phosphorylation and stabilization in prostate cancer by cyclin-dependent kinase 1. *Proc Natl Acad Sci USA*. 2006;103(43):15969-74.
5. UK CR. Prostate cancer survival statistics UK 2018. https://www.cancerresearchuk.org/health-professional/cancer-statistics/statistics-by-cancer-type/prostate-cancer/survival
6. Thorpe LM, Yuzugullu H, Zhao JJ. PI3K in cancer: divergent roles of isoforms, modes of activation and therapeutic targeting. *Nat Rev Cancer*. 2015;15(1):7-24.
7. Majumder PK, Sellers WR. Akt-regulated pathways in prostate cancer. *Oncogene*. 2005;24(50):7465-7474.
8. Cheng I, Witte JS, Jacobsen SJ, et al. Prostatitis, sexually transmitted diseases, and prostate cancer: the California men's health study. *PLOS One*. 2010;5(1):e8736.
9. Bai WK, Zhang W, Hu B. Vascular endothelial growth factor suppresses dendritic cells function of human prostate cancer. *Onco Targets Ther*. 2018;11:1267-1274.
10. Miyara M, Sakaguchi S. Natural regulatory T cells: mechanisms of suppression. *Trends Mol Med*. 2007;13(3):108-116.
11. Kärjä V, Aaltomaa S, Lipponen P, Isotalo T, Talja M, Mokka R. Tumour-infiltrating lymphocytes: a prognostic factor of PSA-free survival in patients with local prostate carcinoma treated by radical prostatectomy. *Anticancer Res*. 2005;25(6C):4435-4438.
12. Vidotto T, Koti M, Squire J. *In Silico Analysis Shows that PTEN Loss and AR Overexpression are Associated with Increased CD8+ T-cell and Treg Density and Earlier Disease Recurrence in Prostate Cancer. AACR*. Chicago, USA: Cancer Research; 2018.
13. Ritchie ME, Phipson B, Wu D, et al. limma powers differential expression analyses for RNA-sequencing and microarray studies. *Nucleic Acids Res*. 2015;43(7):e47.
14. Gu Z, Eils R, Schlesner M. Complex heatmaps reveal patterns and correlations in multidimensional genomic data. *Bioinformatics*. 2016;32(18):2847-2849.
15. Yu G, Wang LG, Han Y, He QY. clusterProfiler: an R package for comparing biological themes among gene clusters. *OMICS*. 2012;16(5):284-287.
16. Yu G, He QY. ReactomePA: an R/Bioconductor package for reactome pathway analysis and visualization. *Mol BioSyst*. 2016;12(2):477-479.
17. Davidsson S, Fiorentino M, Andrén O, et al. Inflammation, focal atrophic lesions, and prostatic intraepithelial neoplasia with respect to risk of lethal prostate cancer. *Cancer Epidemiol Biomarkers Prev*. 2011;20(10):2280-2287.
18. Ripple MO, Hagopian K, Oberley TD, Schatten H, Weindruch R. Androgen-induced oxidative stress in human LNCaP prostate cancer cells is associated with multiple mitochondrial modifications. *Antioxid Redox Signal*. 1999;1(1):71-81.
19. Mizokami A, Gotoh A, Yamada H, Keller ET, Matsumoto T. Tumor necrosis factor-alpha represses androgen sensitivity in the LNCaP prostate cancer cell line. *J Urol*. 2000;164(3 Pt 1):800-805.
20. Ammirante M, Luo JL, Grivennikov S, Nedospasov S, Karin M. B-cell-derived lymphotoxin promotes castration-resistant prostate cancer. *Nature*. 2010;464(7286):302-305.
21. Karin M. NF-kappaB as a critical link between inflammation and cancer. *Cold Spring Harb Perspect Biol*. 2009;1(5):a000141.
22. Karakiewicz PI, Benayoun S, Bégin LR, et al. Chronic inflammation is negatively associated with prostate cancer and high-grade prostatic intraepithelial neoplasia on needle biopsy. *Int J Clin Pract*. 2007;61(3):425-430.
23. Yli-Hemminki TH, Laurila M, Auvinen A, et al. Histological inflammation and risk of subsequent prostate cancer among men with initially elevated serum prostate-specific antigen (PSA) concentration in the Finnish prostate cancer screening trial. *BJU Int*. 2013;112(6):735-741.
24. Overman MJ, McDermott R, Leach JL, et al. Nivolumab in patients with metastatic DNA mismatch repair-deficient or microsatellite instability-high colorectal cancer (CheckMate 142): an open-label, multicentre, phase 2 study. *Lancet Oncol*. 2017;18(9):1182-1191.
25. McDermott DF, Sosman JA, Sznol M, et al. Atezolizumab, an anti-programmed death-ligand 1 antibody, in metastatic renal cell carcinoma: long-term safety, clinical activity, and immune correlates from a phase Ia study. *J Clin Oncol*. 2016;34(8):833-842.
26. Sciarra A, Gentilucci A, Silvestri I, et al. Androgen receptor variant 7 (AR-V7) in sequencing therapeutic agents for castratrion resistant prostate cancer: a critical review. *Medicine*. 2019;98(19):e15608.
27. De Nunzio C, Kramer G, Marberger M, et al. The controversial relationship between benign prostatic hyperplasia and prostate cancer: the role of inflammation. *Eur Urol*. 2011;60(1):106-117.
28. Leung JK, Sadar MD. Non-genomic actions of the androgen receptor in prostate cancer. *Front Endocrinol*. 2017;8:2.
29. Filomeni G, Rotilio G, Ciriolo MR. Disulfide relays and phosphorylative cascades: partners in redox-mediated signaling pathways. *Cell Death Differ*. 2005;12(12):1555-1563.
30. Cargnello M, Roux PP. Activation and function of the MAPKs and their substrates, the MAPK-activated protein kinases. *Microbiol Mol Biol Rev*. 2011;75(1):50-83.
31. Wegiel B, Bjartell A, Culig Z, Persson JL. Interleukin-6 activates PI3K/Akt pathway and regulates cyclin A1 to promote prostate cancer cell survival. *Int J Cancer*. 2008;122(7):1521-1529.
32. Veeranki S. Role of inflammasomes and their regulators in prostate cancer initiation, progression and metastasis. *Cell Mol Biol Lett*. 2013;18(3):355-367.

33. Sun Y, Guo Y. Expression of Caspase-1 in breast cancer tissues and its effects on cell proliferation, apoptosis, and invasion. *Oncol Lett*. 2018; 15(5):6431-6435.
34. Hu B, Elinav E, Huber S, et al. Inflammation-induced tumorigenesis in the colon is regulated by caspase-1 and NLRC4. *Proc Natl Acad Sci USA*. 2010;107(50):21635-21640.
35. Steiner GE, Newman ME, Paikl D, et al. Expression and function of pro-inflammatory interleukin IL-17 and IL-17 receptor in normal, benign hyperplastic, and malignant prostate. *Prostate*. 2003;56(3):171-182.
36. Gooden MJ, de Bock GH, Leffers N, Daemen T, Nijman HW. The prognostic influence of tumour-infiltrating lymphocytes in cancer: a systematic review with meta-analysis. *Br J Cancer*. 2011;105(1): 93-103.
37. Patnaik A, Swanson KD, Csizmadia E, et al. Cabozantinib eradicates advanced murine prostate cancer by activating antitumor innate immunity. *Cancer Discov*. 2017;7(7):750-765.
38. Ali HR, Provenzano E, Dawson SJ, et al. Association between CD8+ T-cell infiltration and breast cancer survival in 12,439 patients. *Ann Oncol*. 2014;25(8):1536-1543.
39. Jansen CS, Prokhnevska N, Master VA, et al. An intra-tumoral niche maintains and differentiates stem-like CD8 T cells. *Nature*. 2019; 576(7787):465-470.
40. McMenamin ME, Soung P, Perera S, Kaplan I, Loda M, Sellers WR. Loss of PTEN expression in paraffin-embedded primary prostate cancer correlates with high Gleason score and advanced stage. *Cancer Res*. 1999;59(17):4291-4296.
41. Taylor BS, Schultz N, Hieronymus H, et al. Integrative genomic profiling of human prostate cancer. *Cancer Cell*. 2010; 18(1):11-22.

SUPPORTING INFORMATION

Additional supporting information may be found online in the Supporting Information section.

How to cite this article: McAllister M, Constâncio V, Patek S, et al. Inflammatory infiltration is associated with AR expression and poor prognosis in hormone naïve prostate cancer. *The Prostate*. 2020;80:1353–1364. https://doi.org/10.1002/pros.24064